Available online at www.sciencedirect.com

ScienceDirect

Catalysis Today 131 (2008) 360–366

CATALYSIS TODAY

www.elsevier.com/locate/cattod

Distinct oxidation behaviors of π-bonded and di-σ-bonded propylene on Ag(1 1 1)

Weixin Huang [a,*], Zhiquan Jiang [a], J.M. White [b]

[a] *Hefei National Laboratory for Physical Sciences at the Microscale and Department of Chemical Physics, MPG-CAS Partner Group of Fritz-Haber-Institut der MPG, University of Science and Technology of China, Hefei 230026, China*

[b] *Department of Chemistry and Biochemistry, Center for Materials Chemistry, University of Texas at Austin, Austin, TX 78712, USA*

Available online 26 November 2007

Abstract

We have investigated the propylene oxidation on Ag(1 1 1) by means of temperature-programmed reaction spectroscopy (TPRS) and reflection-absorption infrared spectroscopy (RAIRS). Existence of atomic oxygen on the surface greatly enhances the interaction of propylene with Ag(1 1 1) at 100 K. With the coverage of oxygen adatoms increasing, a gradual transition from the π-bonded propylene to the di-σ-bonded propylene was observed. Only a small fraction of oxygen adatoms participate the propylene oxidation reaction. Three propylene oxidation pathways were observed, leading to the formation not only of combustion products (CO_2) but also of partially oxidation products (CO and acetone). RAIRS results evidence the formation of hydroxyls on the surface at elevated temperatures. Both TPRS and RAIRS results reveal that the π-bonded and di-σ-bonded propylene follow different combustion mechanisms.

Keywords: Propylene oxidation; Ag(1 1 1); Temperature-programmed reaction spectroscopy; Reflection-absorption infrared spectroscopy

1. Introduction

The epoxidation of olefins is an important type of catalytic process in industry and receives long and extensive studies. The ultimate goal of the catalytic process is to realize the direct epoxidation of olefins using molecular oxygen with high activity and selectivity. The epoxidation of ethylene over silver catalyst is an example of success, and therefore, much research has been devoted to gain a better understanding of the epoxidation mechanism [1–4]. Besides ethylene, silver were also reported to selectively catalyze the epoxidation of styrene, 3,3-dimethylbutene, norbornene, and butadiene [5–7]. However, propylene, butene, and pentene are epoxidized on silver with extremely low selectivity [8–13].

The lower epoxidation selectivity for propylene is generally attributed to the facile abstraction of active allylic hydrogen atoms in propylene by oxygen, which leads to the combustion, but various mechanisms have been postulated [8,13–17]. Cant and Hall proposed the preliminary formation of an intermediate that is common to propylene epoxidation and combustion [8]. Carter and Goddard used the general valence bond (GVB) method to calculate the elementary steps for the olefin oxidation on the silver surface, and suggested that the possible reaction mechanism for the propylene combustion be due to the formation of alkoxide intermediate [14]. Experimental support comes from an infrared spectroscopic study identifying adsorbed acolein intermediate [12]. In contrast, Madix and coworkers employed temperature-programmed reaction spectroscopy (TPRS) to study the propylene oxidation on Ag(1 1 0) and proposed an allylic intermediate formed by the activation of the allylic C–H bond via an acid–base reaction responsible for the propylene combustion [15,16]. This mechanism is further supported later by a theoretical study using dipped adcluster mode (DAM) [17].

Despite a tough task, the pursue for the catalyst for propylene epoxidation by molecular oxygen never stops, and major efforts have been still devoted to the various silver-based catalysts [18–24], and later to copper- and gold-based catalysts [25,26]. However, the related fundamental studies are still poorly limited to several reports on the propylene oxidation on Ag(1 1 0) studied by TPRS, in which only carbon dioxide, water, and surface carbon were detected as

* Corresponding author. Fax: +86 551 3600437.
E-mail address: huangwx@ustc.edu.cn (W. Huang).

0920-5861/$ – see front matter © 2007 Elsevier B.V. All rights reserved.
doi:10.1016/j.cattod.2007.10.045

the oxidation products of propylene oxidation [15,16,27]. The propylene oxidation on Ag(1 1 1), the predominant crystal face present in supported Ag catalysts and powders, has never been studied. Recently, we have investigated the propylene adsorption on clean and oxygen-covered Ag(1 1 1) surfaces [28–30]. In the present paper, we reported the experimental results on propylene oxidation on Ag(1 1 1) studied with temperature-programmed reaction spectroscopy(TPRS) and reflection-absorption infrared spectroscopy (RAIRS). Depending on the oxygen coverage, both π-bonded and di-σ-bonded propylene form on the surface. The propylene oxidation on Ag(1 1 1) behaves quite different from that on Ag(1 1 0). The oxidation products include not only combustion products (CO_2) but also partially oxidation products (CO and acetone). Both TPRS and RAIRS results reveal that the π-bonded and di-σ-bonded propylene follow different combustion mechanisms.

2. Experimental

The experiments were performed in a two-level stainless steel chamber with a base pressure of 2.0×10^{-10} Torr [28]. The upper level is equipped with a Nicolet Magna-IR 860 spectrometer for reflection adsorption infrared spectroscopy (RAIRS), a SRS RGA 200 for residual gas analysis, and an ion sputtering gun; the lower level comprises a UTI-100 quadrupole mass spectroscopy for temperature-programmed reaction spectroscopy (TPRS), and a single-pass cylindrical mirror analyzer for Auger electron spectroscopy (AES).

The Ag(1 1 1) sample was mounted on a tungsten loop attached to rectangular cross section copper bars that were thermally connected to, but electrically isolated from, a hollow copper block filled with liquid nitrogen. The sample temperature was measured by a type K thermocouple inserted into the edge of the crystal and was controlled 80 and 900 K with a commercial temperature controller. The Ag(1 1 1) surface was cleaned by repeated cycles of sputtering at room temperature followed by annealing to 780 K until no contaminants could be detected by AES.

Temperature-programmed reaction experiments were conducted at a ramp rate of 2 K s^{-1}. On the basis of their fragmentation patterns, eight signals, accounting for propene (m/e = 41), carbon dioxide (m/e = 44), water (m/e = 18), carbon monoxide (m/e = 28), oxygen (m/e = 32), acetone (m/e = 43), acrolein (m/e = 56), and epoxypropane (m/e = 58), were monitored simultaneously during the course of TPRS. Using a mercury–cadmium telluride (MCT) detector, RAIRS spectra were collected by co-adding 1500 scans at 4 cm^{-1} resolution. We chose the RAIRS of oxygen-covered Ag(1 1 1) as references for the spectra of propylene adsorbed on oxygen-covered Ag(1 1 1).

Due to the extremely low dissociative sticking coefficient of O_2 on Ag(1 1 1) [31], NO_2 was used to prepare atomic oxygen on Ag(1 1 1), which has been described in detail elsewhere [32]. In this method, NO_2 was dosed at 508 K to form adsorbed O and gas phase NO, a process saturating at a 0.5 monolayer (ML) of atomic oxygen [33]. After the desirable oxygen coverage was prepared, the sample was evacuated and cooled to 100 K prior to the propylene exposure.

3. Results and discussion

Fig. 1a presents the TPRS spectra of propylene following an exposure of 0.25 L (1 L = 1.33×10^{-6} mbar s) propylene on O(a)-covered Ag(1 1 1) with various atomic oxygen coverages (θ_O) at 100 K. On the clean Ag(1 1 1) surface, the propylene desorption spectrum is dominated by a peak at 123 K accompanied by a broad shoulder at 150 K, corresponding to the desorption of physisorbed multilayer and the chemisorbed π-bonded propylene, respectively [28]. With 0.086 ML θ_O pre-covered on the surface, a much more intense π-bonded propylene desorption peak appears at 150 K and there is no desorption peak at 123 K. The π-bonded propylene desorption peak shifts to higher desorption temperature with θ_O increasing. When θ_O is 0.433 ML, the π-bonded propylene desorbs at 181 K; additionally, a shoulder desorption peak arises at 224 K. The desorption peak at 224 K does not move with increasing θ_O, but its intensity overwhelms that of the π-bonded propylene

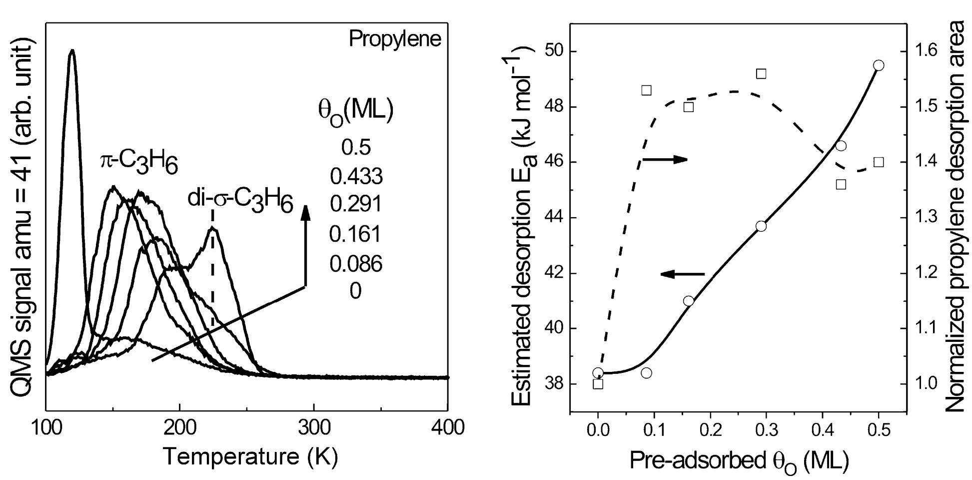

Fig. 1. TPRS spectra of C_3H_6 after a dose of 0.25 L C_3H_6 on O(a)-covered Ag(1 1 1) at 100 K, and the dependence of the desorption barrier of π-bonded propylene and the desorption amount of propylene on the coverage of O(a).

desorption peak at 192 K when the Ag(1 1 1) surface is pre-saturated by O(a) ($\theta_O = 0.5$ ML). On the basis of the RAIRS results (shown below), the desorption peak at 224 K corresponds to the desorption of di-σ-bonded propylene from the O(a)-covered Ag(1 1 1) surface.

The above TPRS results of propylene clearly demonstrate that atomic oxygen on Ag(1 1 1) greatly influences the adsorption of propylene on Ag(1 1 1). Fig. 1b shows the variations of the desorption activation energy of π-bonded propylene and the normalized desorption peak area of propylene as the function of the atomic oxygen coverage. First, pre-covered O_a greatly enhances the chemisorption sticking coefficient of propylene on Ag(1 1 1). At a given exposure of 0.25 L propylene, the propylene desorption peak area from 0.086 ML O_a-covered Ag(1 1 1) is about as 1.5 times as that from the bare Ag(1 1 1), indicating an 1.5-time enhancement of the sticking coefficient. It is noteworthy that both physisorbed and chemisorbed propylene desorb from bare Ag(1 1 1) whereas only chemisorbed propylene from O_a-covered Ag(1 1 1). Therefore the enhancement factor of the chemisorption sticking coefficient of propylene on Ag(1 1 1) should be larger than 1.5. Secondly, the desorption activation energy of the π-bonded propylene increases gradually with the increasing O_a coverage, suggesting the strengthening of the propylene–Ag(1 1 1) interaction. A Readhead analysis [34] assuming first order desorption with a pre-exponential factor of 10^{13} estimates the activation energy for the π-bonded propylene desorption from clean Ag(1 1 1) to be 38.4 kJ mol^{-1}, 1, which eventually reaches 49.5 kJ mol^{-1} at 0.5 ML θ_O. The di-σ-bonded propylene desorbs from Ag(1 1 1) with a θ_O-independent activation energy of 58.1 kJ mol^{-1}.

Experimental results of vibrational spectroscopy confirm the nature of the π-bonded and di-σ-bonded propylene on O(a)-covered Ag(1 1 1). Fig. 2 shows the RAIRS spectra of 0.25 L propylene adsorbed on O(a)-covered Ag(1 1 1) with selective θ_O at 100 K followed by annealing at indicated temperatures. The positive features arising at ca. 975 cm^{-1} are due to Ag-O related vibrations because we chose the RAIRS spectrum foe O(a)-covered Ag(1 1 1) as the reference spectrum. On the basis of TPRS results, only π-bonded propylene forms after propylene adsorption at 100 K for the θ_O below 0.433 ML. Thus the vibrational spectra observed for $\theta_O = 0.086$ and 0.291 ML after adsorption at 100 K account for π-bonded propylene species (curves a in Fig. 2A and B). When θ_O increases to 0.5 ML, the vibrational spectrum after adsorption at 100 K accounts for both π-bonded and di-σ-bonded propylene, however, on the basis of TPRS results, annealing the surface at 200 K desorbs the π-bonded propylene whereas the di-σ-bonded propylene remains on the surface. Therefore, the vibrational spectrum after annealing at 200 K corresponds to the di-σ-bonded propylene (curve b in Fig. 2C), and the difference spectrum between the spectrum after adsorption at 100 K (curve a in Fig. 2C) and that after annealing at 200 K (curve b in Fig. 2C) represents the π-bonded propylene formed on 0.5 ML-O(a)-covered Ag(1 1 1) at 100 K. The observed vibrational features can be unambiguously assigned to the π-bonded and di-σ-bonded propylene on O(a)-covered Ag(1 1 1), which has been discussed in detail in our previous paper [29]. The absence of the feature around 1575 cm^{-1} corresponding to the C=C stretch vibration clarify the nature of the species desorbing from the surface at 224 K to be the di-σ-bonded propylene (curve b in Fig. 2C).

Consistent with the TPRS results, the vibrational frequency of the C=C bond of adsorbed propylene also demonstrates that pre-adsorbed atomic oxygen strengthens the interactions between chemisorbed propylene and the substrate. The vibrational frequency of the C=C bond of the π-bonded propylene red-shifts continuously from 1620 for clean Ag(1 1 1) [28] to 1577 for 0.5 ML-O(a)-covered Ag(1 1 1). This demonstrates a gradual strengthening interaction between the π-bonded propylene and the substrate, subsequently leading to a gradual activation of the C=C double bond of the π-bonded propylene. And eventually the C=C bonds of some chemisorbed propylene are broken, forming the di-σ-bonded propylene at $\theta_O = 0.5$ ML. Ab initio calculations suggest that atomic oxygen creates Ag surface sites with a partial positive charge facilitating electron donation [35]. Thus the propylene π system donates electron more strongly to the silver surface when oxygen atoms create partial positive charge, as suggested elsewhere [15].

Figs. 3 and 4 displays the desorption traces of water, CO_2, CO, acetone, and epoxypropane following an exposure of 0.25 L propylene on O(a)-covered Ag(1 1 1) with various θ_O at 100 K, respectively. The desorption of these products are all reaction-controlled. No acrolein (m/e = 56) desorption was observed. But oxygen desorption peak always appeared (results not shown), and inferred from the comparison between the oxygen desorption amounts from clean Ag(1 1 1) and from C_3H_6(a) co-adsorbed Ag(1 1 1), only a small fraction of initial atomic oxygen react with chemisorbed propylene. For example, only 16% of the initial 0.086 ML atomic oxygen was consumed for 0.25 L propylene oxidation [30]. Very interestingly, propylene oxidation on Ag(1 1 1) produces not only the combustion product (CO_2) but also the partial oxidation product (CO and acetone), although the latter seems to be a minor reaction pathway. But propylene oxidation on Ag(110) have been reported to form only combustion products (CO_2 and H_2O) [15,16,27]. This essential difference illustrates the silver crystal plane likely plays a key role in determining the selectivity of propylene oxidation, and Ag(1 1 1) behaves a higher selectivity for partial oxidation than Ag(1 1 0). Our results suggest that the exposed (1 1 1) crystal plane be responsible for the formation of partial oxidation products during realistic catalytic propylene oxidation over silver-based catalysts.

Roughly, the water desorption peak can be divided into three regions on the basis of the desorption temperature T: I $T < 370$ K; II $370\text{ K} < T < 450$ K; III $524\text{ K} < T < 620$ K, among which the region I is dominant. The reaction-controlled evolution of water is θ_O-dependent. For region I, when θ_O is 0.086 ML, the water desorption peaks appear at 274 and 324 K; with the increasing θ_O, the peak at 324 K intensifies at the dispense of that at 274 K; however, when θ_O increases to 0.5 ML, a strong water desorption arises at 178 K and other two

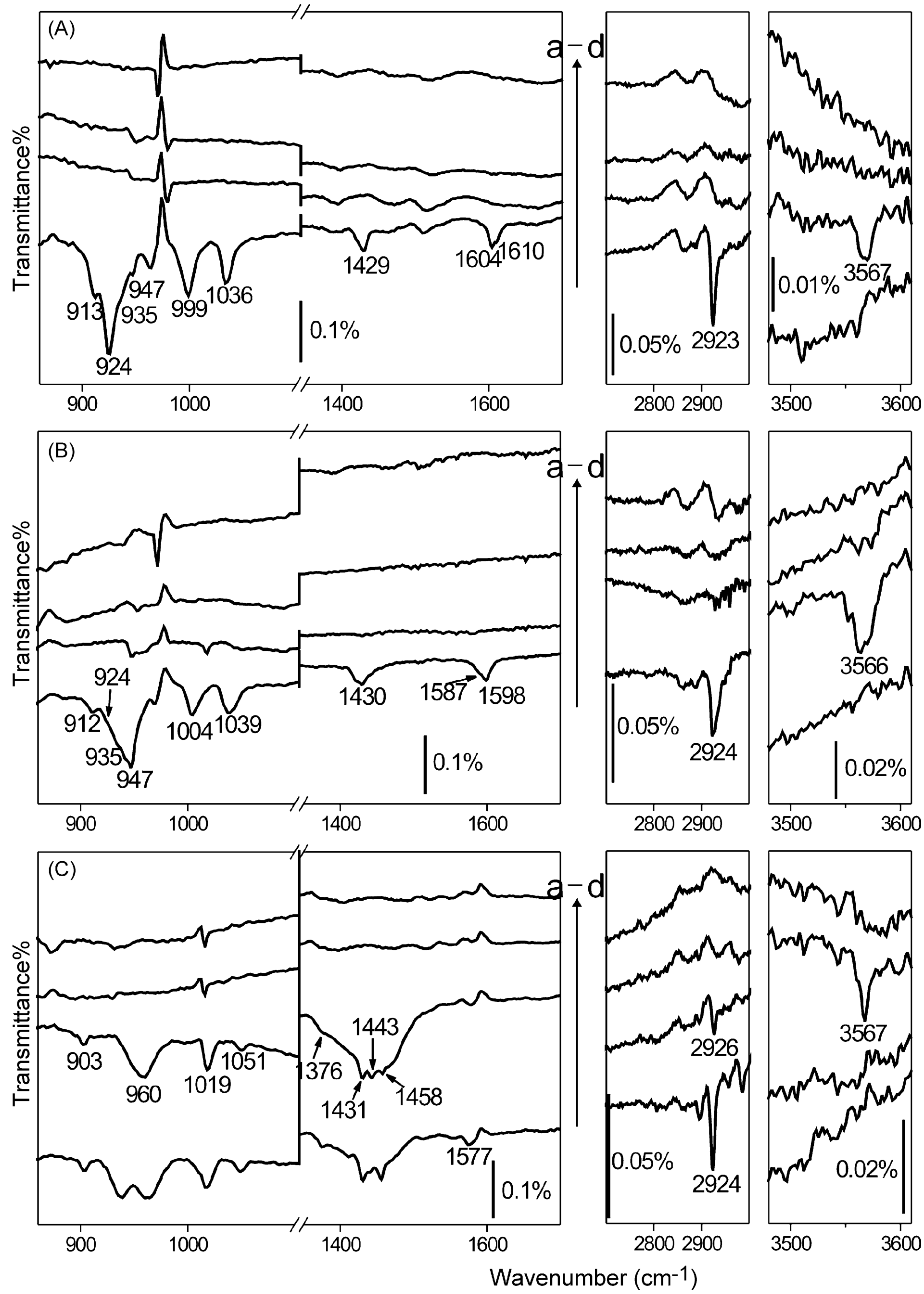

Fig. 2. RAIRS spectra after a dose of 0.25 L C_3H_6 to O(a)-covered Ag(1 1 1) with various O(a) coverages at 100 K (curve a) followed by annealing at 200 K (curve b), 300 K (curve c), and 400 K (curve d), respectively. The atomic oxygen coverage is: (A) 0.086 ML; (B) 0.291 ML; (C) 0.5 ML. All spectra were recorded at 100 K.

peaks at 274 and 324 K. The water evolutions corresponding to regions II and III suggest that H-containing species should exist on the surface at those temperatures. The CO_2 evolution can also be roughly divided into three regions: major desorption peaks at 348 and 381 K (region I), a weak peak around 450 K (region II), and another weak peak around 575 K (region III). The partial oxidation product CO shows a weak peak whose position is slightly θ_O-dependent. The evolution of acetone is θ_O-sensitive, which appears only after the propylene was exposed to the 0.086 and 0.5 ML O(a)-covered Ag(1 1 1) surfaces. Inferred from the peak shape and peak position of the desorption peaks of CO and acetone, the evolutions of CO and acetone follow the same reaction pathway. Finally we would like to point out that the desorption trace of epoxypropane was observed occasionally at 575 K (Fig. 4, $\theta_O = 0.433$ ML). But it is uncertain to conclude that propylene oxidation on Ag(1 1 1) will form epoxypropane. Further experimental results, particularly the TPRS results for different surface stoichiometry of propylene and atomic oxygen with constant θ_O, are needed.

The above TPRS results suggest three oxidation pathways for propylene oxidation on Ag(1 1 1): (1) a dominant combustion route leading to the major desorption peaks of water and CO_2; (2) a minor partial oxidation route forming acetone, whose further oxidation gives rising to the desorption

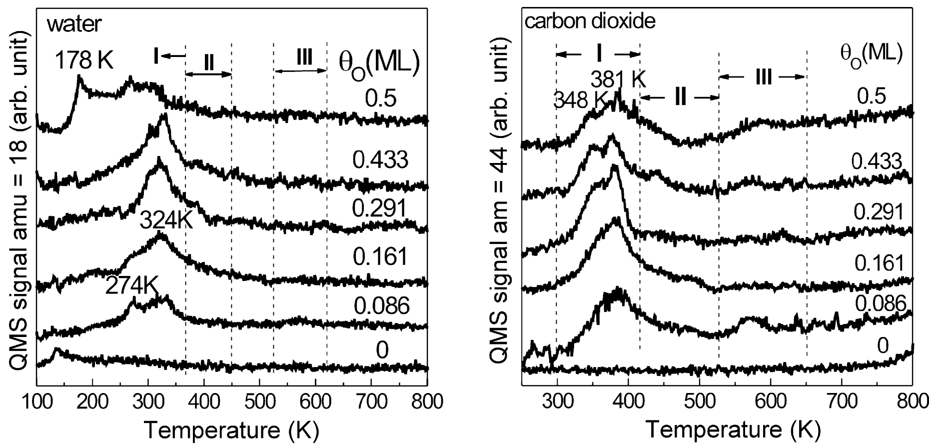

Fig. 3. TPRS spectra of water and CO_2 after a dose of 0.25 L C_3H_6 on O(a)-covered Ag(1 1 1) at 100 K.

peaks of CO, CO_2, and water. It can be seen that the desorption peak of water at 400 K are more intense in the absence of acetone desorption trace ($\theta_O = 0.161$, 0.291, and 0.433 ML) than those when acetone desorption traces appear ($\theta_O = 0.086$ and 0.5 ML); (3) a second minor partial oxidation route (intermediates unknown) eventually producing CO_2 and water desorbing at the highest temperature. This route might also accounts for the epoxypropane formation. These three-oxidation routes have been previously proposed to be the propylene oxidation mechanisms over silver by theoretical calculations [17].

The RAIRS spectra were examined after the O(a)-covered Ag(1 1 1) surface exposed to propylene at 100 K had been annealed to various temperatures (Fig. 2), but failed to provide any information on the likely hydrocarbon intermediates for propylene oxidation. For propylene partial oxidation (the minor reaction routes), the concentrations of involved intermediates might be too low to be detected by RAIRS, because the intermediates should remain on the surface until they undergo further oxidation or desorption that occurs at ca. 400 K and even higher temperatures. But the case is different for the dominant combustion reaction route. As shown in Fig. 2A, after the 0.086 ML-O(a) covered Ag(1 1 1) surface exposed to 0.25 L C_3H_6 at 100 K was annealed at 200 K, the vibrational features corresponding to the π-bonded propylene disappear, consistent with the TPRS results that the π-bonded propylene desorbs from the surface below 200 K. However, a vibrational peak appears at 3567 cm^{-1}, assigned to the stretch vibration of surface hydroxyls. The vibrational peak of hydroxyls disappears after the surface was further annealed at 300 K. Coincidently, dominant water desorption peaks arise in the corresponding TPRS spectrum. These observations demonstrate that observed surface hydroxyls react to produce the water formation in the dominant combustion pathway, i.e., the surface hydroxyls are an intermediate of the combustion pathway. The fact that no hydrocarbon fragments were detected by RAIRS accompanying the formation of surface hydroxyls strongly suggests that the intermediates in the propylene combustion mechanism are surface carbon and hydroxyls, which are further oxidized to produce CO_2 and water. These results evidence that the π-bonded propylene combustion on Ag(1 1 1) follows the same mechanism as that on Ag(1 1 0) established by Madix and coworkers [15,16]: the initial step is an acid–base reaction between O(a) and an allylic C–H bond, resulting in the formation of a surface hydroxyl group and a chemisorbed allyl species; the allyl species decomposes rapidly into surface carbon otherwise it should be detected by RAIRS; finally surface hydroxyls disproportionate to form gaseous water and regenerate O(a), and surface carbon is oxidized to form gaseous CO_2.

Above combustion mechanism holds for the π-bonded propylene combustion on O(a)-covered Ag(1 1 1) with theθ_O

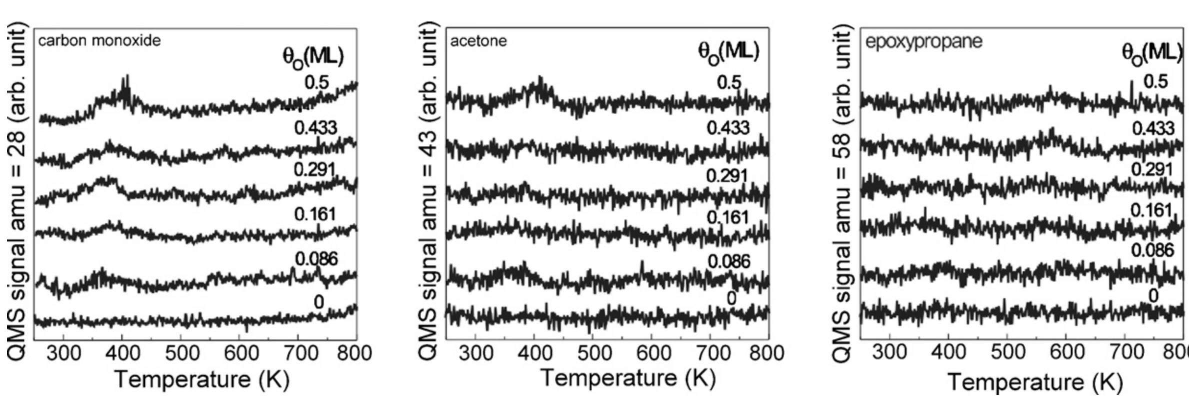

Fig. 4. TPRS spectra of CO, acetone, and epoxypropane after a dose of 0.25 L C_3H_6 on O(a)-covered Ag(1 1 1) at 100 K.

up to 0.433 ML. TPRS results show that higher θ_O prefers the water desorption at 324 K, which could be tentatively attributed to the stabilization of surface hydroxyls by O(a) [36]. However, the combustion pattern changes after an exposure of 0.25 L propylene to 0.5 ML-O(a)-covered Ag(1 1 1) in which the di-σ-bonded propylene dominates the surface. Although the CO_2 evolution does not show much difference, the water evolution does. A strong water desoprtion peak arises at 178 K, far lower that that observed for the π-bonded propylene. The RAIRS did not detect the surface hydroxyls after the surface was annealed at 200 K, which could be rationalized in that the formed surface hydroxyls reacted to produce water desorbing at 178 K. Interestingly, further annealing the surface at 300 K gives rise to the surface hydroxyls that disappear after annealing the surface at even higher temperature (400 K). These observations demonstrate that the di-σ-bonded propylene follows a different combustion route from the π-bonded propylene on Ag(1 1 1). The acidity of the weakly π-bonded propylene is the same for gas-phase propylene, in which the allylic H is most acidic because of the stabilizing effect of the allyl anion (the conjugate base), therefore, the combustion is initiated by the abstract of the allylic H by atomic oxygen [15,16]. But in the di-σ-bonded propylene, the orbitals are rehybridized and the stabilizing factor disappears for the conjugate base. Consequently, the allylic H is no longer the most acidic nor the most reactive toward reactions with O(a). It has been proposed that the combustion of the di-σ-bonded propylene is initiated by the vinylic C–H bond activation on Pd(1 0 0)-c(2 × 2)-O [37,38]. In our case, it is very likely that, inferred from the shape, the broad peak between 1320 and 1550 cm^{-1} in curve b, Fig. 2C includes the vibrational peaks for the hydrocarbon intermediates besides the assigned peaks for the di-σ-bonded propylene. But it is unlikely to make any clear assignment.

Since water desorption is controlled by the surface hydroxyls disproportionation reaction, the water evolution at 178 K indicate that the surface hydroxyls disproportionate more facile on the O(a)-covered Ag(1 1 1) surfaces with 0.5 ML θ_O than those with a lower θ_O. This might be related to the θ_O-dependent surface structure of atomic oxygen on Ag(1 1 1). At low coverages, individual oxygen adatoms randomly adsorbed on the surface; adding oxygen adatoms led to nucleation and rapid growth of islands of surface oxide; and eventually, a continuous well-ordered surface oxide film with a p (4 × 4)-O unit cell formed at saturation coverage (0.5 ML) [39]. On a continuous well-ordered surface oxide film, the surface hydroxyls could disproportionate to form water with a low barrier due to the relatively facile of the proton migration within hydroxyls. After the desorption of the resulted water at 178 K, the continuous oxide film is broken and consequently, the remained surface hydroxyls react to form water at 274 and 324 K, the same as the cases when the pre-adsorbed atomic oxygen is below 0.5 ML.

Our results report for the first time that propylene oxidation on Ag(1 1 1) can produce partial oxidation products, particularly acetone, under appropriate conditions. The formation of acetone was previously reported for propylene oxidation on Rh(1 1 1)-p(2 × 1)-O [40]. The acetone is a product of the central carbon attack followed by a H-migration step, as suggested by theoretical calculations [17].

4. Conclusions

We have investigated the propylene oxidation on Ag(1 1 1) by means of temperature-programmed reaction spectroscopy (TPRS) and reflection-absorption infrared spectroscopy (RAIRS). Propylene is weakly π-bonded to clean Ag(1 1 1) at 100 K. Pre-adsorbed atomic oxygen strongly enhances the interaction of propylene with Ag(1 1 1). With the coverage of atomic oxygen increasing, the C=C double bond of the π-bonded propylene is gradually activated and eventually the di-σ-bonded propylene forms on the surface. Three propylene oxidation pathways are observed: a dominant combustion route leading to the formation of water and CO_2; a minor partial oxidation route forming acetone, whose further oxidation gives rising to the desorption peaks of CO, CO_2, and water; another minor partial oxidation route (intermediates unknown) eventually producing CO_2 and water. Our results report for the first time that propylene oxidation on Ag(1 1 1) can produce partial oxidation products, particularly acetone, under appropriate conditions. The π-bonded propylene undergoes combustion initiated by the abstraction of allylic hydrogen by atomic oxygen whereas the di-σ-bonded propylene follows a different combustion mechanism.

Acknowledgements

This work is financially supported by National Natural Science Foundation of China (20503027) and the ‘‘Hundred Talent Program’’ of Chinese Academy of Sciences.

References

[1] X.E. Verykios, F.P. Stein, R.W. Coughlin, Catal. Rev. Sci. Eng. 22 (1980) 197.
[2] W.M.H. Sachtler, C. Backx, R.A. van Santen, Catal. Rev. Sci. Eng. 23 (1981) 127.
[3] R.A. van Santen, H.P.C. Kuipers, Adv. Catal. 35 (1987) 265.
[4] K.A. Jørgensen, Chem. Rev. 89 (1989) 431.
[5] S. Hawker, C. Mukoid, J.P.S. Badyal, R.M. Lambert, Surf. Sci. 219 (1989) L615.
[6] C. Mukoid, S. Hawker, J.P.S. Badyal, R.M. Lambert, Catal. Lett. 4 (1990) 57.
[7] J.T. Robert, R.J. Madix, J. Am. Chem. Soc. 110 (1988) 8540.
[8] N.W. Cant, W.K. Hall, J. Catal. 52 (1978) 81.
[9] M. Imachi, M. Egashira, R.L. Kuczkowski, N.W. Cant, J. Catal. 70 (1981) 177.
[10] M.F. Portela, C. Henriques, M.J. Pires, L. Ferreria, M. Baerna, Catal. Today 1 (1987) 101.
[11] P.V. Geenen, H.J. Boss, G.T. Pott, J. Catal. 77 (1982) 499.
[12] I.L.C. Freriks, R. Bouwman, P.V. Geenen, J. Catal. 65 (1980) 311.
[13] M. Akimoto, K. Ichikawa, E. Echigoya, J. Catal. 76 (1982) 333.
[14] E.A. Carter, W.A. Goddard III, Surf. Sci. 209 (1989) 243.
[15] M.A. Barteau, R.J. Madix, J. Am. Chem. Soc. 105 (1983) 344.
[16] J.T. Robert, R.J. Madix, W.W. Crew, J. Catal. 141 (1993) 300.
[17] Z.M. Hu, H. Nakai, H. Nakatsuji, Surf. Sci. 401 (1998) 371.
[18] B. Cooker, A.M. Gaffney, J.D. Jewson, W.H. Onimus, US Patent 5,965,480 (1999).
[19] G.Z. Lu, X.B. Zuo, Catal. Lett. 58 (1999) 67.
[20] A.L. de Oliveira, A. Wolf, F. Schuth, Catal. Lett. 73 (2001) 157.

[21] J.Q. Lu, M.F. Luo, C. Li, Appl. Catal. A 237 (2002) 11.
[22] R.P. Wang, X.W. Guo, X.S. Wang, J.Q. Hao, Catal. Lett. 90 (2003) 57.
[23] G.J. Jin, G.Z. Lu, Y.L. Guo, Y. Guo, J.S. Wang, X.L. Liu, W.Y. Kong, X.H. Liu, Catal. Lett. 97 (2004) 191.
[24] A. Takahashi, N. Hamakawa, I. Nakamura, T. Fujitani, Appl. Catal. A 294 (2005) 34.
[25] M. Haruta, M. Date, Appl. Catal. A 222 (2001) 427.
[26] R.M. Lambert, F.J. Williams, R.L. Cropley, A. Palermo, J. Mol. Catal. A 228 (2005) 27.
[27] J.T. Ranney, S.R. Bare, Surf. Sci. 382 (1997) 266.
[28] W.X. Huang, J.M. White, Surf. Sci. 513 (2002) 399.
[29] W.X. Huang, J.M. White, Langmuir 18 (2002) 9622.
[30] W.X. Huang, J.M. White, Catal. Lett. 84 (2002) 143.
[31] C.T. Campbell, Surf. Sci. 157 (1985) 43.
[32] W.X. Huang, J.M. White, Surf. Sci. 529 (2003) 455.
[33] S.R. Bare, K. Griffiths, W.N. Lennard, H.T. Tang, Surf. Sci. 342 (1995) 185.
[34] P.A. Redhead, Vacuum 12 (1962) 203.
[35] J.A. Rodriquez, C.T. Campbell, Surf. Sci. 206 (1988) 426.
[36] S.W. Jorgensen, A.G. Sault, R.J. Madix, Langmuir 1 (1985) 526.
[37] X.-C. Guo, R.J. Madix, J. Am. Chem. Soc. 117 (1995) 5523.
[38] X.-C. Guo, R.J. Madix, Surf. Sci. 391 (1997) L1165.
[39] C.I. Carlisle, T. Fujimoto, W.S. Sim, D.A. King, Surf. Sci. 470 (2000) 15.
[40] X. Xu, C.M. Friend, J. Am. Chem. Soc. 113 (1991) 6779.